Supporting Information

A field portable electrochemical immunosensor based on multifunctional $Ag_2O/g\text{-}C_3N_4$ @MA-DBB covalent organic framework receptor interface for single-step detection of aflatoxin M_1 in raw milk samples

Iram Naz[a,b], Akhtar Hayat*[b], Farhat Jubeen*[a], Sadia Asim[a], Abida Kausar[a],

a. Department of Chemistry, Govt. College Women University, Arfa Kareem Road Faisalabad, 38000, Pakistan
b. Interdisciplinary Research Center in Biomedical Materials (IRCBM), COMSATS University Islamabad, Lahore Campus, 1.5 Km Defense Road, off Raiwind Road, Lahore, Punjab, Pakistan 54000

*Corresponding author: akhtarhayat@cuilahore.edu.pk ; dr.farhatjubeen@gcwuf.edu.pk

Table S1. FT-IR spectra frequencies of $g\text{-}C_3N_4$, $Ag_2O/g\text{-}C_3N_4$-COOH, MA-DBB-COF and $Ag_2O/g\text{-}C_3N_4$-COOH@MA-DBB-COF

Wavelength (cm^{-1})	Assignment
3729-3723	υ(NH)
2936-2912	δCH_2
1684-1620	υ(Ar-C=N)
1535-1506-1402-1392,1307,1226	υ(C-N) heterocycle
1130-1024	υ(C-N)
770	ω(C-N)
804	Triazine Unit

υ: stretching, δ: bending, ω: wagging

Table S2. Raman spectrum for D-band and G-band of g-C_3N_4, Ag_2O/g-C_3N_4-COOH, MA-DBB-COF and Ag_2O/g-C_3N_4-COOH@MA-DBB-COF

Material	D band wavenumber cm^{-1}	G band wavenumber cm^{-1}	I_D/I_G
g-C_3N_4	800	1530	0.5
Ag_2O/g-C_3N_4	1470	1803	0.81
MA-DBB-COF	-	1705	-
Ag_2O/g-C_3N_4-COOH@MA-DBB-COF	1273	1617	0.78

Table S3. Thermal degradation steps of g-C_3N_4, Ag_2O/g-C_3N_4-COOH, MA-DBB-COF and Ag_2O/g-C_3N_4-COOH@MA-DBB-COFwith respect to changes in temperature

Material	Thermal degradation temperature range (°C), and % weight loss				
	I	II	III	IV	V
g-C_3N_4	123-149 1	559-681 87.7	681-800 0.1	-	-
Ag_2O/g-C_3N_4-COOH	48-98 2	129-154 0.34	154-800 0	-	-
MA-DBB-COF	72-150 19	150-393 51	390-450 4	507-561 2	555-800 0.1
Ag_2O/g-C_3N_4-COOH@MA-DBB-COF	100-185 10	223-454 11	506-692 7.3	692-800 0.1	-

Table S4. Electro active surface area and peak potential difference of bare PGE and at different modification steps of PGE,

Electrodes	**Active Surface Area (cm^2)**	**ΔE_p**
*Bare	0.024	0.46
EDC-NHS/Ag_2O/g-C_3N_4+COF	0.031	0.38
anti-AFM_1 antibody/EDC-NHS/Ag_2O/ g-C_3N_4+COF	0.021	0.31
BSA/anti-AFM_1 antibody/ EDC-NHS/Ag_2O/g-C_3N_4+COF	0.020	0.44
AFM_1/BSA/ anti-AFM_1 antibody/ EDC-NHS/Ag_2O/g-C_3N_4+COF	0.018	0.16

*Geometric area of PGE is 0.052

Table S5: Analytical performance comparison of the BSA/anti-AFM_1 antibody/EDC-NHS/Ag_2O/g-C_3N_4-COOH@MA-DBB-COF/PGE immunosensor with recently literature reported electrochemical sensors for detection of AFM_1.

Sr. no	Electrode	Materials	Linear range	Detection limit	References
1	Screen printed carbon electrode	Anti-idiotype nanobodies	0.25-5 ng/mL	0.09 ng/mL	[1]
2	Screen printed carbon electrode	MoS_2 QD@UiO-66-NH_2 composite	0.2-10 ng/mL	0.06 ng/mL	[2]
3	Screen printed carbon electrode	PEG/Gold nanoparticles composite	0.02-0.3 ng/mL	0.007 ng/mL	[3]
4	Screen printed carbon electrode	GO–CS/CeO_2–CS nanocomposite	0.01-1 ng/mL	0.009 ng/mL	[4]
5	Dispense printed electrodes	Single-walled carbon nanotubes (SWCNTs)	0.01-1 ng/mL	0.02 ng/mL	[5]
6	Pencil graphite electrode	rGO/Gold nanoparticles	0.0005-0.8 ng/mL	0.0003 ng/mL	[6]
7	Glassy Carbon electrode	Pt nanoparticles loaded on Fe-MOF	0.01-80 ng/mL	0.002 ng/mL	[7]
8	Glassy Carbon electrode	Polyaniline	0.005-0.09 ng/mL	0.001 ng/mL	[8]
9	Pencil graphite electrode	Ag_2O/g-C_3N_4-COOH@MA-DBB-COF	0.03-1000 fg/mL	0.01 fg/mL	**This work**

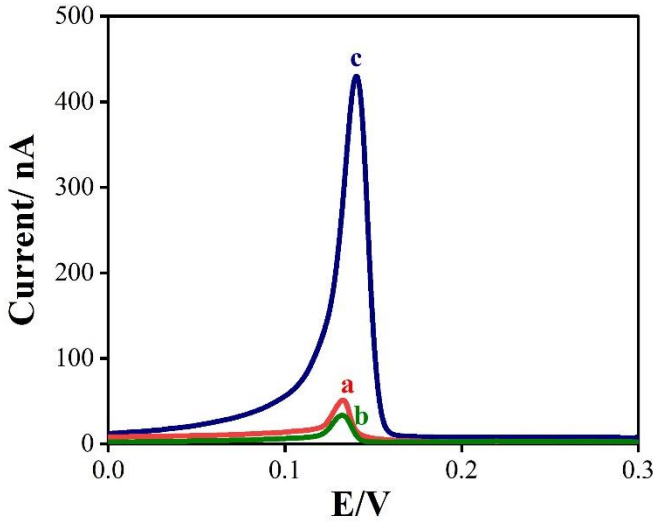

Figure S1: DPV at three steps of (a) pure Ag_2O/g-C_3N_4; (b) Ag_2O/g-C_3N_4-COOH; (c) Ag_2O/g-C_3N_4-COOH@MA-DBB-COF.

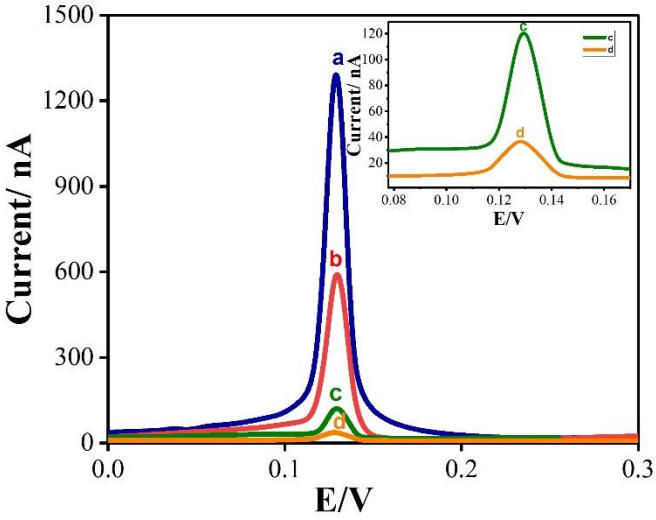

Figure S2: DPV at different steps of; a) Ag_2O/g-C_3N_4-COOH@MA-DBB-COF/EDC-NHS (b) Ag_2O/g-C_3N_4-COOH@MA-DBB-COF/EDC-NHS/ anti-AFM_1 antibody (c)Ag_2O/g-C_3N_4-COOH@MA-DBB-COF+EDC-NHS/ anti-AFM_1 antibody /BSA, and (d) Ag_2O/g-C_3N_4-COOH@MA-DBB-COF/EDC-NHS/ anti-AFM_1 antibody /BSA/AFM_1.

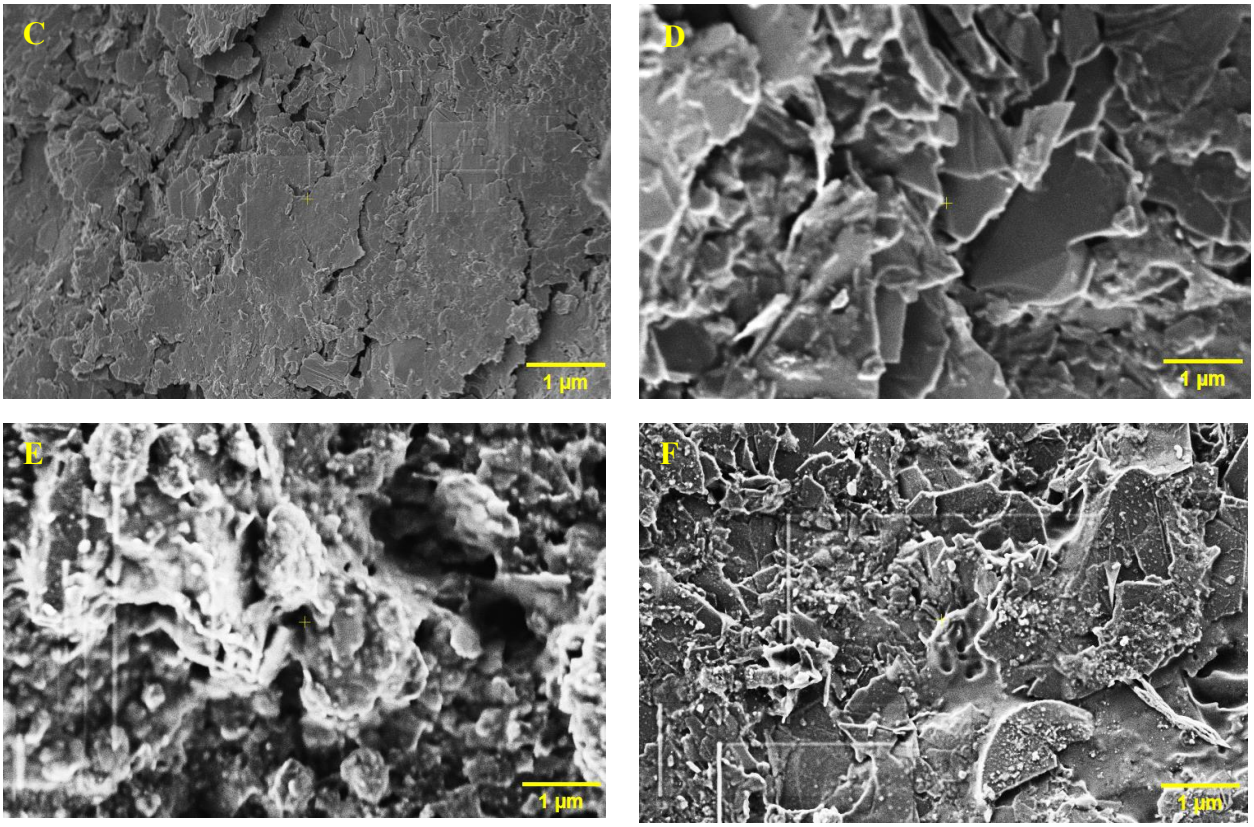

Figure S3: FE-SEM images of step wise modification of PGE for; (C) bare electrode, (D) EDC-NHS/Ag_2O/g-C_3N_4-COOH@MA-DBB-COF/PGE, (E) anti-AFM_1antibody/EDC-NHS/Ag_2O/g-C_3N_4-COOH@MA-DBB-COF/PGE,(F)BSA/anti-AFM_1antibody/EDC-NHS/Ag_2O/g-C_3N_4-COOH@MA-DBB-COF/PG.

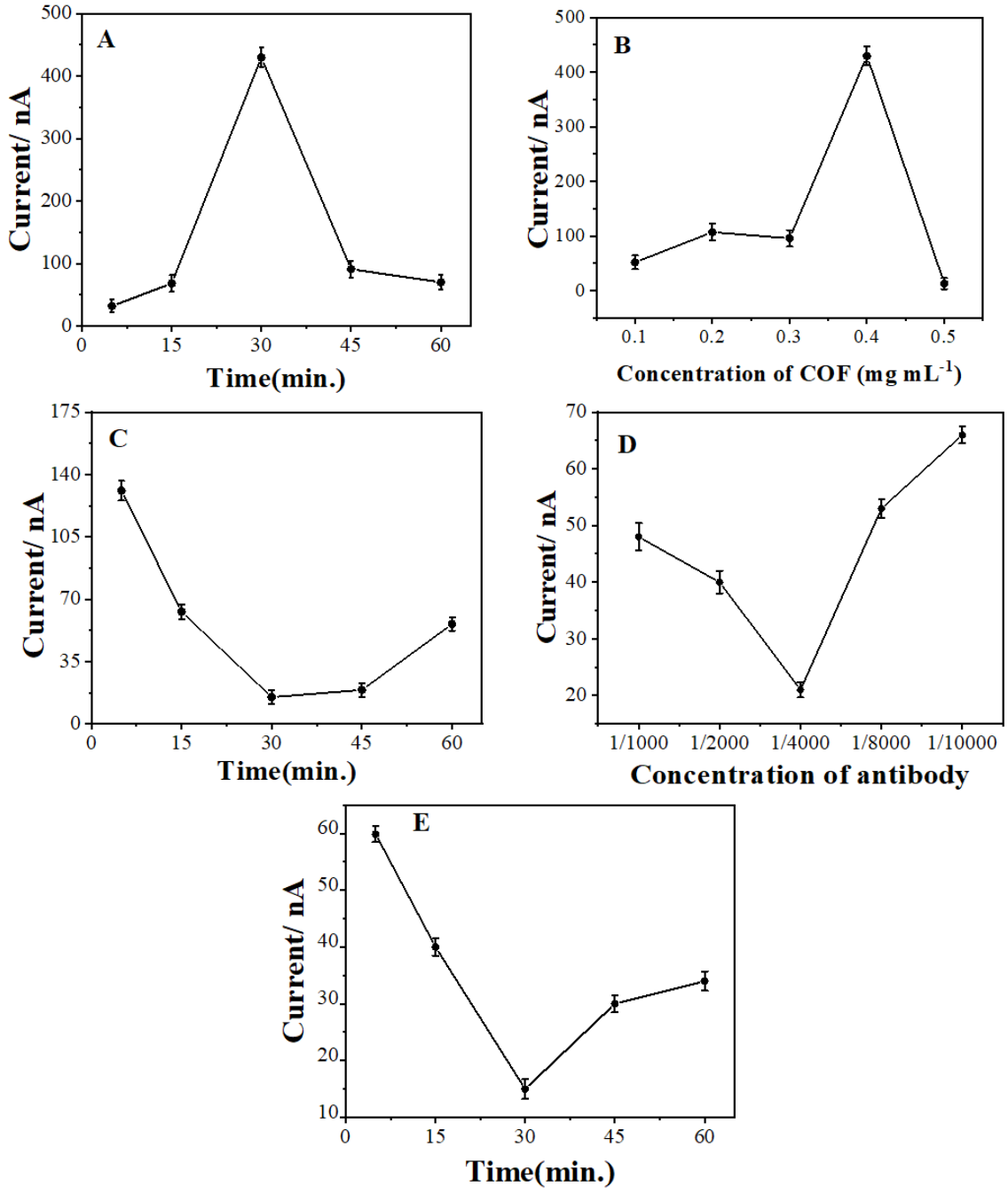

Figure S4: Optimization of the immunosensor: (A) different incubation time of Ag_2O/g-C_3N_4 for 5, 15, 30, 45 and 60min. ; (B) effect of MA-DBB-COF concentration with 0.1, 0.2, 0.3, 0.4 and 0.5 mg mL^{-1}; (C) effect of reaction time of anti-AFM_1 antibody for 5, 15, 30, 45 and 60 min.; (D) effect of the concentration of anti-AFM_1 antibody with 1/1000, 1/2000, 1/4000, 1/8000 and 1/10,000 units of anti-AFM_1 antibody in PBS dilutions and (E) different incubation time of AFM_1 for 5, 15, 30 45 and 60 min.

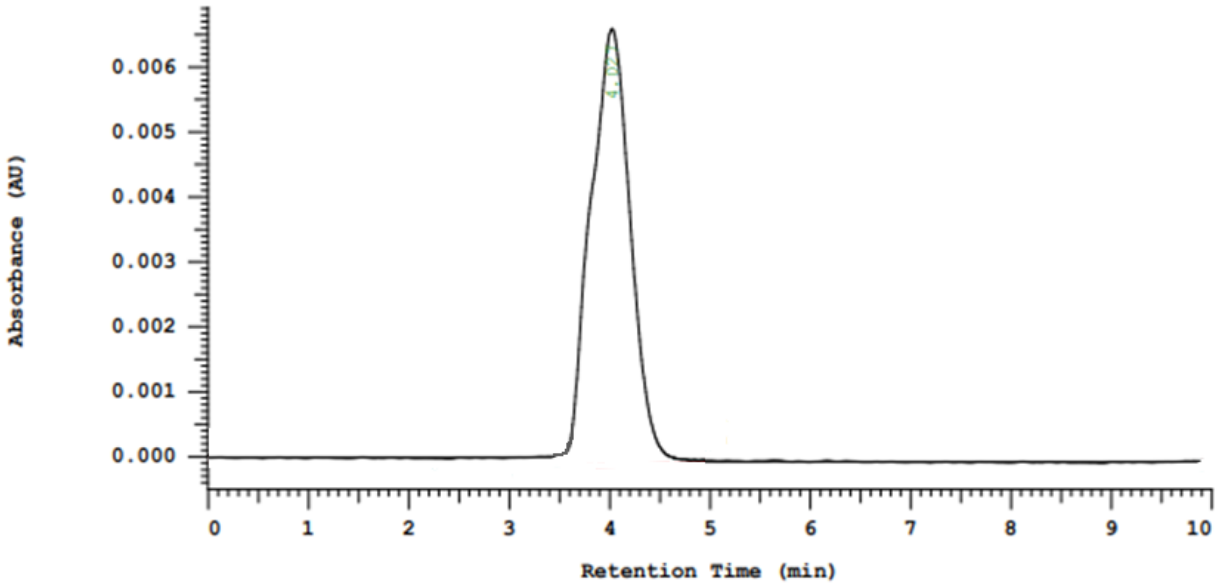

Figure S5: HPLC Chromatogram of standard AFM_1.

References

1. X. Tang, G. Catanante, X. Huang, J.-L. Marty, H. Wang, Q. Zhang and P. Li, *Food Chemistry*, 2022, **383**, 132598.
2. G. Kaur, S. Sharma, S. Singh, N. Bhardwaj and A. Deep, *ACS omega*, 2022, **7**, 17600-17608.
3. M. Hamami, A. Mars and N. Raouafi, *Microchemical Journal*, 2021, **165**, 106102.
4. X. An, X. Shi, H. Zhang, Y. Yao, G. Wang, Q. Yang, L. Xia and X. Sun, *New Journal of Chemistry*, 2020, **44**, 1362-1370.
5. B. D. Abera, A. Falco, P. Ibba, G. Cantarella, L. Petti and P. Lugli, *Sensors*, 2019, **19**, 3912.
6. S. F. Ahmadi, M. Hojjatoleslamy, H. Kiani and H. Molavi, *Food chemistry*, 2022, **373**, 131321.
7. F. Jahangiri–Dehaghani, H. R. Zare and Z. Shekari, *Food Chemistry*, 2020, **310**, 125820.
8. T. Kulikova, A. Porfireva, G. Evtugyn and T. Hianik, *Electroanalysis*, 2019, **31**, 1913-1924.